Supplementary information

Understanding the deformation of IRMOF-1 during carbon dioxide and argon adsorption from hybrid Monte Carlo/molecular dynamics simulations

Lucas J. dos Santos[1], Iuri S. V. Segtovich[2], Amaro G. Barreto Jr.[1], Frederico W. Tavares[1,2*]

[1]EngenHria de Processos Químicos e Bioquímicos (EPQB), Escola de Química, Universidade Federal do Rio de Janeiro, Rio de Janeiro, 21941-909, RJ, Brazil.

[2]Programa de EngenHria Química, COPPE, Universidade Federal do Rio de Janeiro, Rio de Janeiro, 21941-909, RJ, Brazil.

*Corresponding author(s). E-mail(s): tavares@eq.ufrj.br;

Force Field

The force field proposed by Dubbeldam et al. [1] for IRMOF-1 (Fig. 1) represents the Zn_4O cluster using only Lennard-Jones and Coulombic potentials between the individual atoms. In contrast, linker molecules are described using a combination of general force field parameters, including DREIDING [2] and CVFF [3], for bond, bend, and torsion constants:

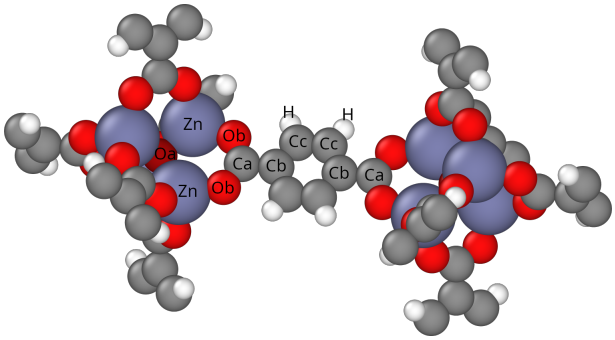

Fig. 1 Definition of the different atom types present in IRMOF-1.

The bond stretching between two bonded atoms is represented by a harmonic potential:

$$V_b(r_{ij}) = \frac{1}{2} k_b (r_{ij} - r_0)^2 \tag{1}$$

The bond-angle vibration between a triplet of atoms is also described by a harmonic potential:

$$V_a(\theta_{ijk}) = \frac{1}{2} k_\theta (\theta_{ijk} - \theta_0)^2 \tag{2}$$

Proper and improper dihedrals are represented by a periodic function:

$$V_d(\phi_{ijkl}) = k_\phi (1 + \cos(m\phi - \phi_s)) \tag{3}$$

where ϕ is the angle between the ijk and the jkl planes. The only difference here compared to what Dubbeldam et al. [1] described is that in the definition of improper dihedral angles of atoms *i-j-k-l*, *i* is the central atom. Additionally, the Lennard-Jones and Coulomb 1-4 interactions were included (with full values).

Table 1 Bond parameters [1]

i	j	k_b (kJ mol^{-1} nm^{-2})	r_0 (nm)
Ob	Ca	452173.73	0.127
Ca	Cb	294124.11	0.144
Cb	Cc	401932.76	0.1365
Cc	Cc	401932.76	0.1365
Cc	H	304309.33	0.095

Table 2 Bend parameters [1]

i	j	k	k_θ (kJ mol^{-1} rad^{-2})	θ_0 (deg)
Ob	Ca	Ob	1130.43	132
Ob	Ca	Cb	456.31	114
Ca	Cb	Cc	290.399	120
Cc	Cb	Cc	753.62	120
Cc	Cc	Cb	753.62	120
Cb	Cc	H	309.82	120
Cc	Cc	H	309.82	120

Table 3 Torsion parameters [1]

i	j	k	l	k_ϕ (kJ mol^{-1})	ϕ_s (deg)	m
Ob	Ca	Cb	Cc	10.467	180	2
Ca	Cb	Cc	H	12.560	180	2
Ca	Cb	Cc	Cc	12.560	180	2
Cb	Cc	Cc	H	12.560	180	2
Cb	Cc	Cc	Cb	12.560	180	2
Cc	Cb	Cc	Cc	12.560	180	2
H	Cc	Cb	Cc	12.560	180	2
H	Cc	Cc	H	12.560	180	2

Table 4 Improper torsion parameters [1]

i	j	k	l	k_ϕ (kJ mol^{-1})	ϕ_s	m
Ca	Cb	Ob	Ob	41.872	180	2
Cb	Cc	Cc	Ca	41.88	180	2
Cc	Cb	Cc	H	1.549	180	2

Table 5 Non-bonded parameters for IRMOF-1 [1]

Atom type	ϵ/k_B (K)	σ (Å)	Charge
Zn	0.42	2.7	1.275
Oa	700	2.98	−1.5
Ob	70.5	3.11	−0.6
Ca	47	3.74	0.475
Cb	47.86	3.47	0.125
Cc	47.86	3.47	−0.15
H	7.65	2.85	0.15

For unlike LJ interactions, the standard Lorentz-Bethelot combining rules are used.

Table 6 Non-bonded parameters for CO_2 [4] and Ar [5]

Atom type	ϵ/k_B (K)	σ (Å)	Charge
C_{CO_2}	27.0	2.80	0.7
O_{CO_2}	70.0	3.05	−0.35
Ar	119.8	3.40	—

For unlike LJ interactions, the standard Lorentz-Bethelot combining rules are used.

Additional results

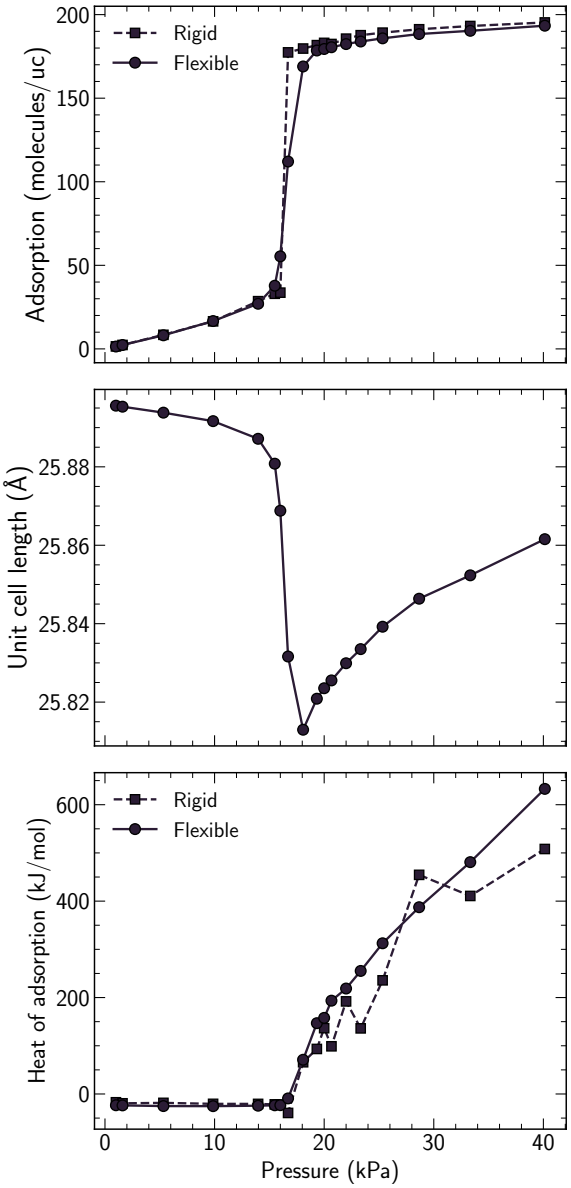

Fig. 2 Adsorption isotherms, strain isotherms, and heats of adsorption of CO_2 on IRMOF-1 at 195 K for $1 \times 1 \times 1$ cells and 12 Å of cutoff radius.

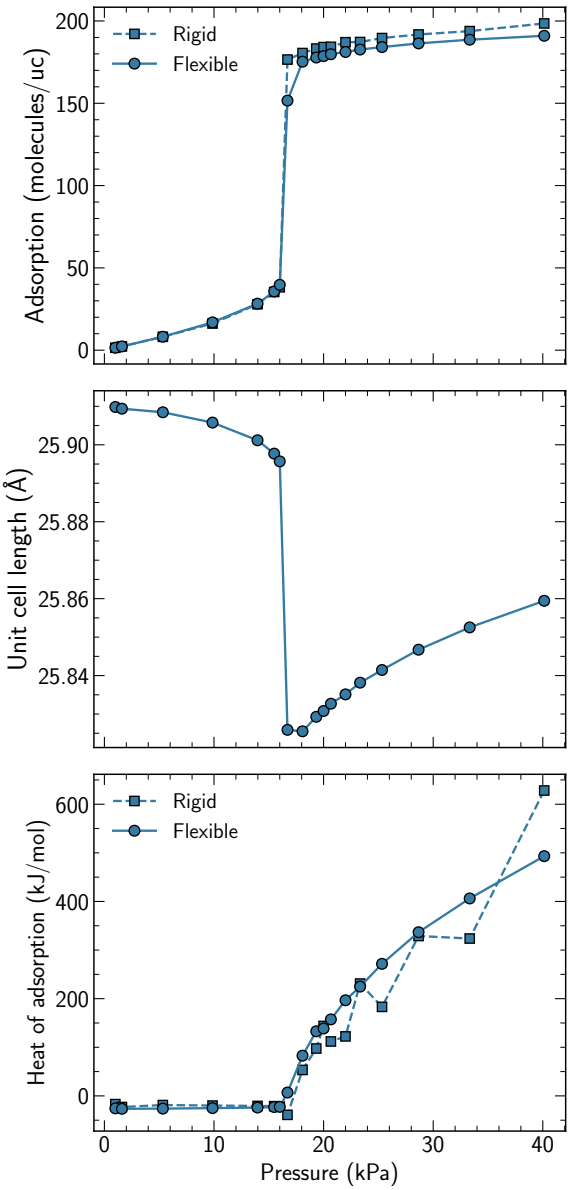

Fig. 3 Adsorption isotherms, strain isotherms, and heats of adsorption of CO_2 on IRMOF-1 at 195 K for $2 \times 2 \times 2$ cells and 12 Å of cutoff radius.

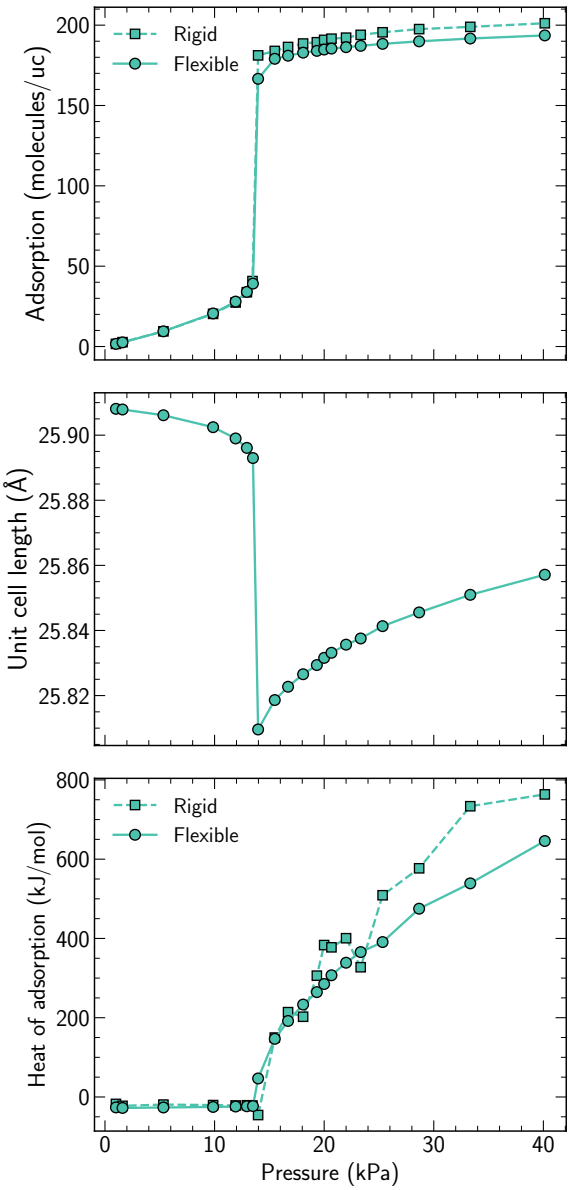

Fig. 4 Adsorption isotherms, strain isotherms, and heats of adsorption of CO_2 on IRMOF-1 at 195 K for $2 \times 2 \times 2$ cells and 14 Å of cutoff radius.

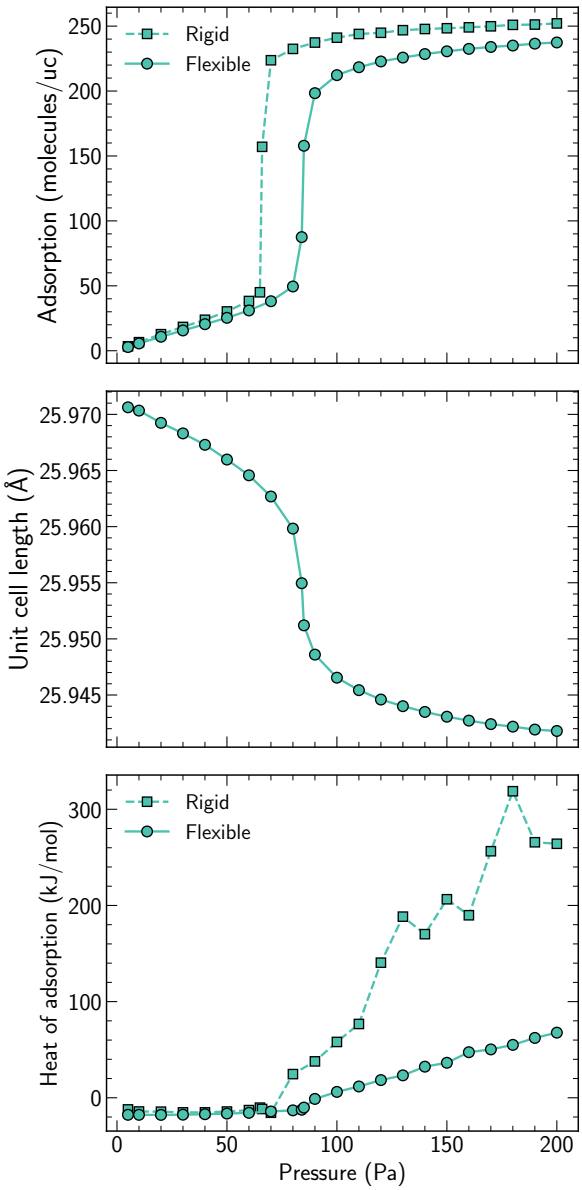

Fig. 5 Adsorption isotherms, strain isotherms, and heats of adsorption of Ar on IRMOF-1 at 78 K for $2 \times 2 \times 2$ cells and 14 Å of cutoff radius.

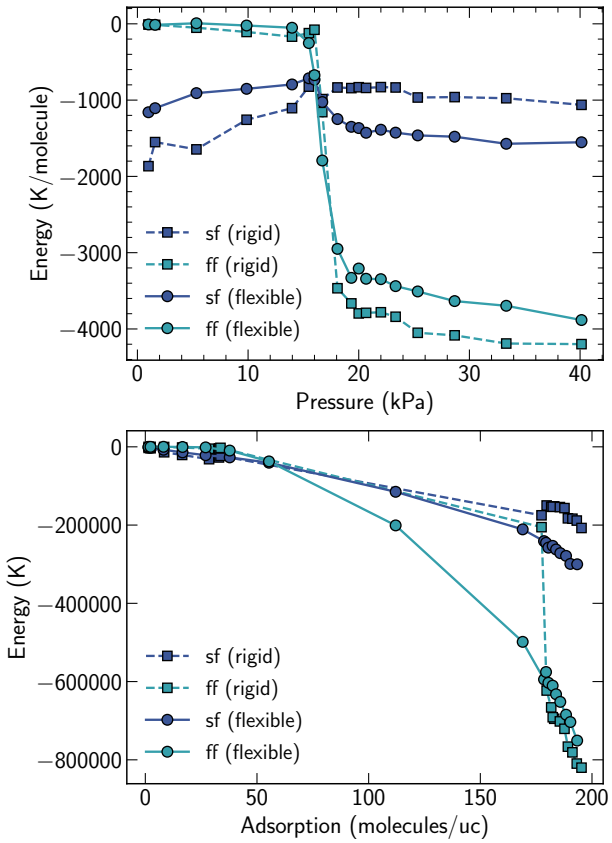

Fig. 6 Fluid-fluid and solid-fluid energy contributions for CO_2 adsorption on IRMOF-1 at 195 K ($1 \times 1 \times 1$ cells and 12 Å of cutoff radius).

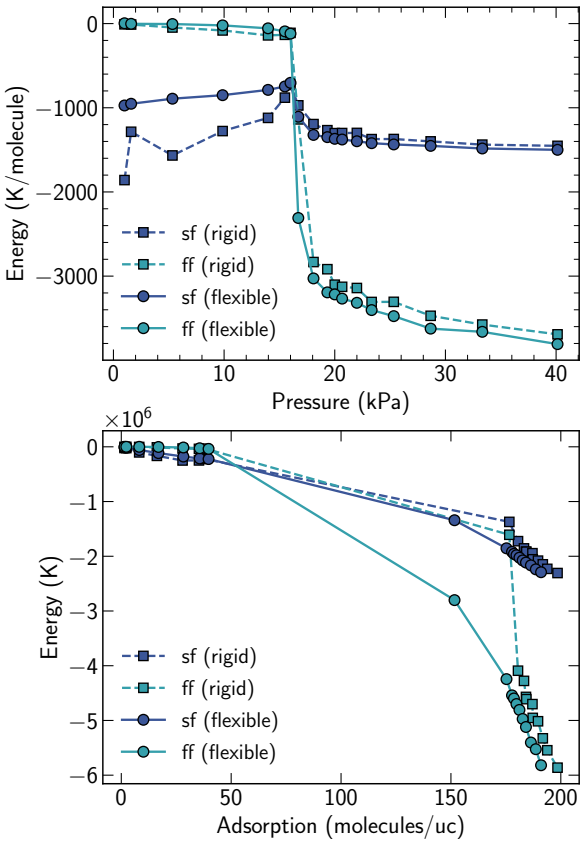

Fig. 7 Fluid-fluid and solid-fluid energy contributions for CO_2 adsorption on IRMOF-1 at 195 K ($2 \times 2 \times 2$ cells and 12 Å of cutoff radius).

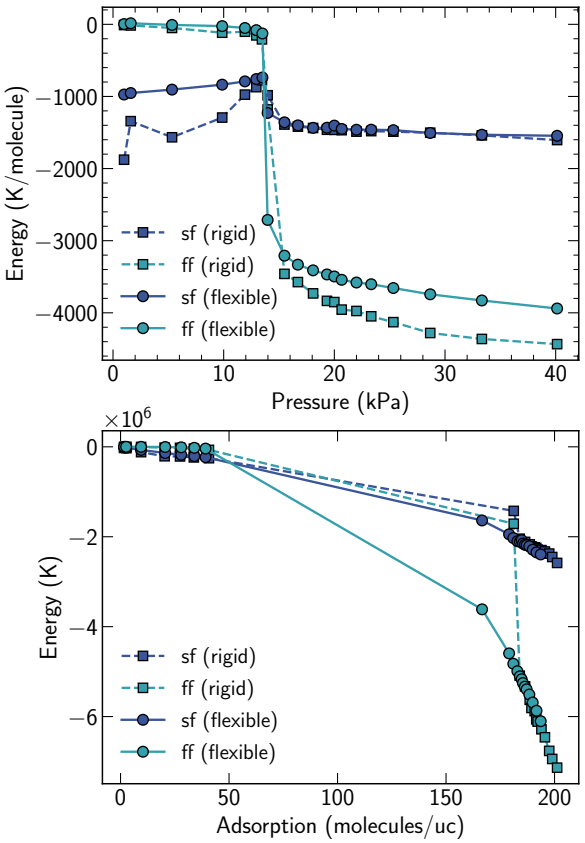

Fig. 8 Fluid-fluid and solid-fluid energy contributions for CO_2 adsorption on IRMOF-1 at 195 K ($2 \times 2 \times 2$ cells and 14 Å of cutoff radius).

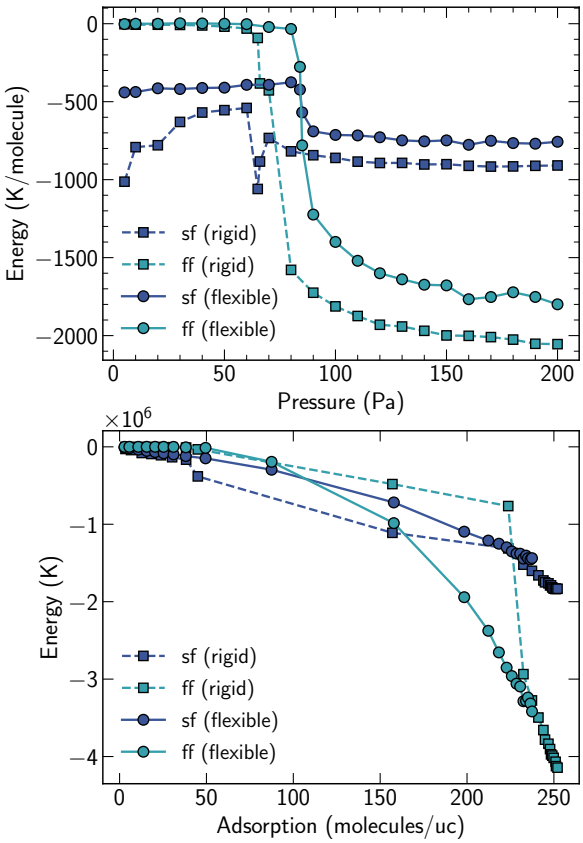

Fig. 9 Fluid-fluid and solid-fluid energy contributions for Ar adsorption on IRMOF-1 at 78 K ($2 \times 2 \times 2$ cells and 14 Å of cutoff radius).

References

[1] Dubbeldam, D., Walton, K.S., Ellis, D.E., Snurr, R.Q.: Exceptional Negative Thermal Expansion in Isoreticular Metal–Organic Frameworks. Angewandte Chemie International Edition **46**(24), 4496–4499 (2007) https://doi.org/10.1002/anie.200700218

[2] Mayo, S.L., Olafson, B.D., Goddard, W.A.: DREIDING: A generic force field for molecular simulations. The Journal of Physical Chemistry **94**(26), 8897–8909 (1990) https://doi.org/10.1021/j100389a010

[3] Lifson, S., Hagler, A.T., Dauber, P.: Consistent force field studies of intermolecular forces in hydrogen-bonded crystals. 1. Carboxylic acids, amides, and the C:O.cntdot..cntdot..cntdot.H- hydrogen bonds. Journal of the American Chemical Society **101**(18), 5111–5121 (1979) https://doi.org/10.1021/ja00512a001

[4] Potoff, J.J., Siepmann, J.I.: Vapor–liquid equilibria of mixtures containing alkanes, carbon dioxide, and nitrogen. AIChE Journal **47**(7), 1676–1682 (2001) https://doi.org/10.1002/aic.690470719

[5] Maitland, G.C., Rigby, M., Smith, E.B., Wakeham, W.A.: Intermolecular Forces: Their Origin and Determination. International series of monographs on chemistry. Clarendon Press, Oxford, U.K. (1981)